JACS
JOURNAL OF THE AMERICAN CHEMICAL SOCIETY

ARTICLE

pubs.acs.org/JACS

Defining CYP3A4 Structural Responses to Substrate Binding. Raman Spectroscopic Studies of a Nanodisc-Incorporated Mammalian Cytochrome P450

Piotr J. Mak,[†] Ilia G. Denisov,[‡] Yelena V. Grinkova,[‡] Stephen G. Sligar,[*,‡,§,#] and James R. Kincaid[*,†]

[†]Department of Chemistry, Marquette University, Milwaukee, Wisconsin 53233, United States

[‡]Department of Biochemistry, [§]Department of Chemistry, and [#]College of Medicine, University of Illinois, Urbana, Illinois 61801, United States

Supporting Information

ABSTRACT: Resonance Raman (RR) spectroscopy is used to help define active site structural responses of nanodisc-incorporated CYP3A4 to the binding of three substrates: bromocriptine (BC), erythromycin (ERY), and testosterone (TST). We demonstrate that nanodisc-incorporated assemblies reveal much more well-defined active site RR spectroscopic responses as compared to those normally obtained with the conventional, detergent-stabilized, sampling strategies. While ERY and BC are known to bind to CYP3A4 with a 1:1 stoichiometry, only the BC induces a substantial conversion from low- to high-spin state, as clearly manifested in the RR spectra acquired herein. The third substrate, TST, displays significant homotropic interactions within CYP3A4, the active site binding up to 3 molecules of this substrate, with the functional properties varying in response to binding of individual substrate molecules. While such behavior seemingly suggests the possibility that each substrate binding event induces functionally important heme structural changes, up to this time spectroscopic evidence for such structural changes has not been available. The current RR spectroscopic studies show clearly that accommodation of different size substrates, and different loading of TST, do not significantly affect the structure of the substrate-bound ferric heme. However, it is here demonstrated that the nature and number of bound substrates do have an extraordinary influence on the conformation of bound exogenous ligands, such as CO or dioxygen and its reduced forms, implying an effective mechanism whereby substrate structure can impact reactivity of intermediates so as to influence function, as reflected in the diverse reactivity of this drug metabolizing cytochrome.

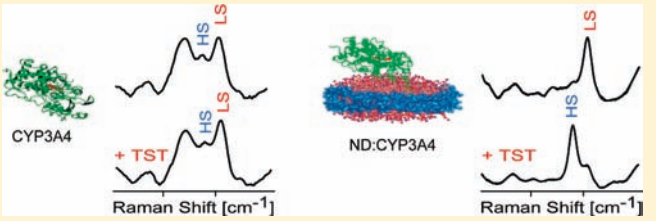

INTRODUCTION

The membrane-bound human cytochrome P450 3A4 (CYP3A4), the most abundant P450 expressed in liver and intestine, is involved in the metabolism of almost 50% of all known pharmaceuticals and is one of the most studied of the 57 human P450s.[1−3] Its large active site can accommodate substrates of diverse sizes, structures, and affinities; depending on substrate size, it is also able to simultaneously bind multiple substrate molecules, a situation that sometimes gives rise to cooperative functional behavior.[3−7] Homotropic cooperativity is observed when an increasing concentration of substrate leads to higher activity and atypical kinetics,[3−7] while heterotropic cooperativity is manifested when binding of an effector or second substrate molecule can impact (stimulate or inhibit) catalytic activity toward a substrate.[3−7]

This ability to accommodate a wide range of substrate structures, yet still retain active site structural constraints adequate to impart regio- and stereoselectivity toward certain substrates,[3−9] implies the existence of a complex interplay between substrate structure and active site structural elements, the understanding of which carries important implications for drug development research.[3−9] The practical significance of this issue, coupled with a relatively small amount of reliable structural data,[10−14] has fueled a large number of computational and modeling studies searching for insight into the structural basis for substrate recognition and manipulation of the inherent reactivity of CYP3A4.[15−17]

Although early crystallographic studies provided useful data for the substrate-free form, efforts to acquire structures for substrate-bound forms were disappointing in that the substrates employed either did not bind to the enzyme or bound in apparently unproductive modes.[10,11] However, recent studies have revealed that binding of ketoconazole and erythromycin (ERY) causes dramatic, but different, changes in protein conformation.[12,13] Specifically, while the active site volume increased by more than 80% in both cases, erythromycin binding resulted in a nonproductive complex, while two ketoconazole molecules are accommodated within the heme active site. These crystallographic data clearly support the position that drug-metabolizing cytochromes P450, such as CYP3A4, possess relatively "malleable" pockets and that its active site structure and reactivity can "adjust" in

Received: July 2, 2010
Published: January 5, 2011

response to substrate structure. Given these observations and the physiological importance of these enzymes, it is evident that the development of successful protocols for application of a solution phase technique capable of faithfully revealing active site structural changes associated with binding of substrates, inhibitors, and heterotropic effectors to mammalian cytochromes P450 is of immense value.

Of the many spectroscopic techniques that have been effectively applied to study heme proteins, resonance Raman (RR) has proven itself to be quite versatile in documenting several types of critical heme site structural changes.[18,19] High frequency marker modes respond to changes in oxidation- or spin-state of the central iron in well-established and documented ways, while low frequency modes indicate changes in protein interactions with the heme periphery.[20−25] This is important, because the presence of the propionic acid and (potentially conjugated) vinyl peripheral substituents has long been considered as possibly important structural determinants of heme reactivity, whose influence may be sensitively manipulated by protein−heme interactions.[23,26−28] Moreover, excitation within the strong Soret band of the heme can lead to efficient enhancement of internal modes of Fe−XY fragments, providing a very effective probe of the key linkages between the heme prosthetic group and exogenous ligands, including the CO molecule[18,19,29−35] and the physiologically relevant dioxygen and bound peroxo- and hydroperoxo fragments.[36−42]

While this powerful spectroscopic technique has long offered great promise for application to mammalian P450s, certain complications have persisted, one of the most problematical being the propensity of these membrane-bound enzymes to aggregate in solution in undefined and uncontrolled ways.[43] In fact, this annoying tendency toward aggregation is a general problem that has plagued all biophysical studies of these systems. Fortunately, the so-called "nanodisc" technology has been developed for use in mammalian cytochrome P450 research, permitting membrane-bound P450 enzymes to be studied in an environment that eliminates aggregation. The nanodisc approach utilizes an encircling amphipathic membrane scaffold protein (MSP), which can stabilize a phospholipid bilayer by forming a kind of "belt" around the hydrophobic core,[44,45] the essential point being that this unique sampling methodology can now be used to permit quite detailed characterization of the structure and function of mammalian P450s in an environment that, for the first time, closely mimics the native environment (Figure 1). In fact, the application of the "nanodisc" technology to mammalian P450 research has already enabled detailed studies of nanodisc-incorporated stoichiometric 1:1 complexes of CYPs and their natural reductases to form functional organized catalytic assemblies.[46−50]

In this Article, attention is focused on the interactions of nanodisc-incorporated CYP3A4 (designated ND:CYP3A4) with three substrates, bromocriptine (BC), erythromycin (ERY), and testosterone (TST), the functional properties for each of which have been thoroughly documented (see Figure 2 for structures). The first of these, BC, is a frequently studied 3A4 inhibitor/substrate that is especially effective in inducing an almost complete change to the high spin (HS) state (∼95%).[46,51] The choice of ERY stems from the fact that, even though it does not induce a substantial spin state conversion (only ∼20% HS), it is used in diagnostics as a test substrate for CYP3A4.[52] Those two substrates bind tightly to the protein in the ratio of 1:1 with dissociation constants of ∼0.15 and ∼120 μM, respectively

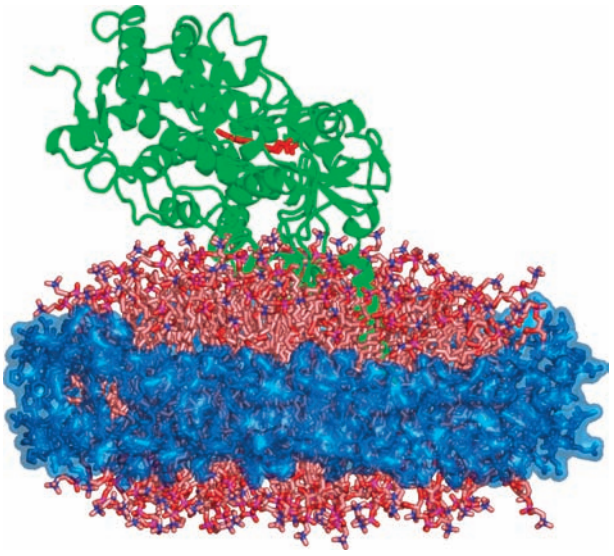

Figure 1. The nanodisc−CYP3A4 asembly. The CYP3A4 molecule is green, cartoon representation, with heme shown in red sticks. Lipids are shown as sticks with nitrogen atoms colored blue and oxygen in red, while the scaffold protein encompassing the lipid bilayer is shown as a blue semitransparent surface with dark blue sticks.

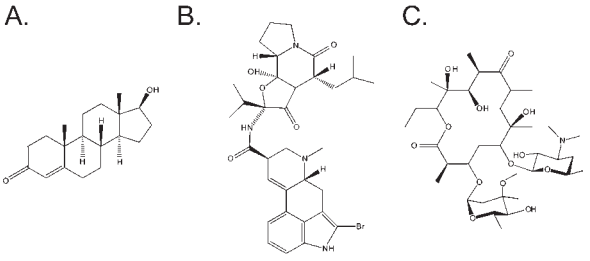

Figure 2. The structures of testosterone (A), bromocriptine (B), and erythromycin (C).

(unpublished results). Testosterone, an important substrate of the steroid hydroxylases, is metabolized by CYP3A4 and has been employed as a useful target for the study of homotropic interactions within CYP3A4,[46,49,50] which can bind up to three molecules of this substrate. In these previous works, it was found that the substrate-free nanodisc assembly is essentially a low spin system, containing only 7% HS component; while binding of the first TST substrate causes a small conversion to HS state and some increase in consumption of NADPH reductant, there is no product formed. Addition of the second substrate causes an almost complete (98%) conversion to a HS state, but still yields rather low (5%) coupling efficiency. Finally, the addition of the third substrate, while not giving significant changes in spin state or turnover rate, does improve coupling (up to 14%). Such observations obviously suggest the likely possibility that each substrate binding event induces functionally important heme structural changes, but up to this time spectroscopic evidence for such structural changes has not been available.

Here, we present data for ferric resting states of the protein, in both the substrate-free and the substrate-bound forms, which show remarkable differences in RR spectra collected for samples prepared in commonly employed detergent and those acquired for ND:CYP3A4; that is, while no substantial effects of substrate binding could be observed in conventional media, quite distinct

spectra were obtained for the substrate-free and substrate-bound forms in these nanodisc assemblies. More importantly, it is evident from the RR data acquired here, for the first time, that the occupation of the distal pocket by multiple substrates does not lead to structurally different high spin states. However, the nature and number of bound substrates do have a substantial influence on the conformation of bound exogenous ligands, an observation that implies that substrate occupation may impact mechanism by influencing the disposition of bound exogenous ligands, such as dioxygen and its reduced (peroxo- and hydroperoxo-) forms.

EXPERIMENTAL SECTION

A. Sample Preparation. 1. Materials. All chemicals were purchased from Sigma Aldrich, with the exception of chelating Sepharose FF and Superdex 200 (GE Healthcare), Coomassie G-250 reagent (Pierce), Emulgen 913 (Karlan Research Products, Santa Rosa, CA), and palmitoyl-oleoyl-phosphatidylcholine (POPC) (Avanti Polar Lipids, Alabaster, AL).

2. Protein Expression and Purification. Cytochrome P450 3A4 was expressed from the NF-14 construct in the PCWori+ vector with a C-terminal pentahistidine tag generously provided by Dr. F. P. Guengerich, as previously described.[53] The presence of the histidine-tag has been shown to not perturb the measured turnover parameters of CYP3A4.[54] Heterologous expression and purification from *E. coli* was carried out using a modified procedure[46] as described in the Supporting Information of ref 55.

3. Preparation of Nanodiscs Incorporated Protein. The application of the nanodisc system for solubilization of integral membrane proteins incorporated into nanoscale bilayers has been described in detail in several publications.[46,56−60] Assembly of human CYP3A4 in nanodiscs was accomplished using the scaffold protein MSP1D1 with the poly(histidine) tag[61] removed as described previously.[46] Briefly, purified CYP3A4 from the *E. coli* expression system was solubilized by 0.1% Emulgen 913 and mixed with the disk reconstitution mixture containing MSP1D1, POPC,[1] and sodium cholate. A molar mixing ratio of 0.1:1:65:130 (CYP3A4:MSP1D1:POPC:cholate) was chosen to favor formation of monomeric CYP3A4 incorporated into nanodiscs with the proper stoichiometry of scaffold protein and lipid. Detergents are removed by absorption on the AmberliteXAD-2 (Sigma Aldrich, Milwaukee, WI), which initiates self-assembly of nanodiscs. Purification of the fraction of nanodiscs with incorporated CYP3A4 was achieved using Ni-NTA affinity column followed by size exclusion chromatography as previously described.[55] The result of this self-assembly reaction is a monomer of CYP3A4 contained in a discoidal POPC bilayer ∼10 nm in diameter stabilized by the encircling amphipathic membrane scaffold protein belt. The CYP3A4-nanodiscs were prepared in substrate-free form and kept at 4 °C. For comparison, spectra also have been measured using CYP3A4 solubilized in 0.1% Emulgen 913.

B. Resonance Raman Measurements. 1. Preparation of Samples for RR Measurements. The concentration of nanodisc-incorporated protein was ∼100 μM, unless otherwise specified. Electronic absorption spectroscopy showed that this incorporated substrate-free (SF) sample contains ∼11% of high spin component, noting, however, that these absorption measurements were performed on samples that were only 10−15 μM in nanodisc concentration.[51] The samples containing the relatively large substrates were prepared by addition of 200 μM bromocryptime (BC) or 800 μM erythromycin (ERY). To investigate the effect of TST loading on the RR spectra, different concentrations of substrate were added to substrate-free samples to give final concentrations of 100, 130, 200, 350, 600, and 1200 μM; the ND:CYP3A4 samples were in 100 mM potassium phosphate buffer, pH 7.4. Concentrated solutions of substrates in methanol-containing buffer solutions, where the final concentration of methanol was always less than 1%, were added to the substrate-free form.

The carbonmonoxy ferrous ND:CYP3A4 samples were prepared in the following manner. Approximately 100 μL of ∼100 μM ferric ND:CYP3A4 sample was placed in a 5 mm NMR tube (WG-5 Economy, Wilmad) and closed with a rubber septum (Sigma-Aldrich, Milwaukee, WI). The tube was connected to a vacuum line via a needle connection, and the sample was degassed by three cycles of alternating application of vacuum and filling with argon gas. Following the final evacuation, CO gas was introduced to the NMR tube, and the ferric sample was reduced by addition of ∼2 mol equiv (∼5 μL)[62] of sodium dithionite dissolved in freshly degassed 100 mM potassium phosphate buffer, pH 7.4.

Samples were also prepared in so-called conventional media, which consisted of 50 mM potassium phosphate, pH 7.4 buffer containing 20% of glycerol, 1 mM DTT, and 0.1% of Emulgen 913 to help ensure solubilization of CYP3A4 as a monomer. The concentration of ferric samples of substrate-free CYP3A4 was 60 μM, and the concentration of testosterone in the substrate-bound sample was 600 μM.

2. Resonance Raman Measurements. The ferric CYP3A4 samples were measured with the 406.7 nm excitation line from a Kr^+ laser (Coherent Innova model 100-K3), while the Fe(II)−CO adducts were excited using the 441.6 nm line provided by a He−Cd laser (Liconix model 4240). The RR spectra of all samples were measured using a Spex 1269 spectrometer equipped with an Andor Newton EMCCD detector (model DU971, Andor Technologies). The slit width was 100 μm, and the 1200 g/mm and 2400 g/mm gratings were used for lower resolution and high resolution measurements, respectively. The laser power at the sample was adjusted to ∼8 mW for ferric samples, while the power of ∼1 mW was maintained for the CO adducts to minimize photodissociation. To avoid laser-induced heating and protein degradation, the samples were contained in spinning NMR tubes (5 mm DO, WG-5 ECONOMY, Wilmad). Measurements were done using a 180° backscattering geometry, and the laser beam was focused onto the sample using a cylindrical lens to form a line image.[63] Spectra were calibrated with fenchone and processed with Grams/32 AI software (Galactic Industries, Salem, NH). Data were obtained at 4 and 30 °C. The sample-containing NMR tube was placed in a homemade quartz Dewar flask filled with water, and the temperature was monitored using a thermocouple and did not change by more than ±2 °C during the measurements.

3. Peak Fitting Procedure. The ν(Fe−CO) bands in the absolute spectra of substrate-free and TS-bound samples exhibit clearly visible asymmetry, implying the presence of several Fe−C−O conformers, an observation that was confirmed by the appearance of distinct ν(C−O) stretches in the high frequency region. To document the fractional population of these multiple Fe−CO conformers, the low frequency RR spectra of ferrous CO adducts were analyzed with Grams 32/AI software using a peak fitting procedure, employing 50/50% Gaussian/Lorentzian functions.[64] The fitting was performed in a manner that restricts the number of peaks to the minimum, noting that this region also contains a well-known heme mode.[24,25] Thus, to obtain satisfactory fitting of Fe−CO envelope, it was necessary to include this feature. First, its frequency (and bandwidth) was derived by fitting of the less complex spectra of the BC and ERY, yielding values of 501 cm^{-1} (15 ± 0.5 cm^{-1}); it is noted that these two fitting operations also produced virtually identical relative intensities with respect to the ν_7 mode at 673 cm^{-1}, as would be expected. Therefore, the parameters of this band, including its intensity relative to the ν_7 mode, were held constant in fitting all of the other (more complex) spectra. The intensities, bandwidths, and frequencies of the peaks associated with the ν(Fe−C) modes in the spectra of the substrate-free sample and of the sample with high concentration of TST were allowed to change during iteration cycles, and it was found that their ν(Fe−C) envelopes were best fitted with two ν(Fe−C) modes, results confirmed by the observation of two ν(C−O) modes in the high frequency region. It is also noted that the ν(C−O) modes in the spectra

of samples with smaller TST concentrations have the same frequencies as the ν(C−O) modes in the spectra of SF sample and sample containing a high concentration of TST. Accordingly, while fitting spectra of those samples containing low amounts of TST, the frequencies of the two ν(Fe−C) modes were kept the same as extracted from the spectra of SF and high concentration TST, while the bandwidths and intensities were allowed to change during iteration cycles. Significantly, it is also noted that (within a given spectrum) the relative intensities of the ν(Fe−C) modes are consistent (within experimental error) with the relative intensities of the two high frequency ν(C−O) modes.

RESULTS AND DISCUSSION

A. Ferric P450 3A4 and Its Interaction with Substrates.

1. Complications Arising from Detergent Solubilization. To document the differences in the RR spectra between CYP3A4 prepared in so-called "conventional" media and that assembled in nanodiscs, two samples of cytochrome CYP3A4 were prepared in detergent solution; as explained in the Experimental Section, these contained Emulgen 913, which is commonly employed for enhancing the solubility of mammalian cytochromes P450.[43,50,64,65] The spectra of the substrate-free enzyme, as well as that bound with 10 mol equiv of testosterone, are shown in Figure 3 (traces A and B, "CM" stands for "conventional media", as opposed to nanodisc-incorporated proteins that are the main subject of this Article). The so-called spin state marker bands in these spectra are expected to occur near 1500 (ν_3), 1590 (ν_2), and 1640 cm^{-1} (ν_{10}) for the LS state and near 1490, 1570, and 1630 cm^{-1} for the HS state.[18,19,23−25,32] As can be readily seen in the top trace, the ν_3 spin state marker bands of the substrate-free state indicate the presence of substantial amounts of both low (1502 cm^{-1}) and high (1488 cm^{-1}) spin components; however, it is noted that the intensity ratio cannot be assumed to be directly proportional to the spin state populations due to differences in inherent RR cross sections. Given this fact, efforts were made here to deduce the relative populations of LS and HS states by establishing the relative RR scattering cross sections of the ν_3 modes from studies of Cytochrome P450$_{cam}$ (CYP101), where it was possible to generate virtually pure HS and LS samples, each containing 0.25 M sulfate ion as an internal standard (the concentration of substrate-free sample was 11.7 μM, and that of the substrate-bound was 11.1 μM); the relative cross sections of the ν_3 mode were determined to be I_{HS}/I_{LS} = 1.23 (unpublished data). This ratio was used to compute the HS and LS popuations for spectra A and B of Figure 3, yielding HS/LS population ratios of 30/70 for both. See Table S1 of the Supporting Information for a summary of calculated spin state distributions for all samples studied in this work. It is noted that the HS components of the ν_2 and ν_{10} modes are not readily observed, because of overlaps with other modes (i.e., ν_{37} and ν(C=C)$_{vinyl}$ modes). Most interestingly, it can be seen that the addition of substrate (testosterone in a 10-fold excess) to this conventionally solubilized protein does not substantially affect the spin state distribution of the enzyme (trace B), a result in stark contrast to results normally obtained for most soluble bacterial cytochromes P450, where binding of typical substrates causes conversion of an almost pure LS state to population having 90−98% HS component.[25,32] The spectroscopic behavior observed here for these detergent-solubilized proteins suggests that the "substrate-free" sample shows some conversion to HS state due to the presence of the Emulgen 913, which has been suggested to be a substrate for mammalian

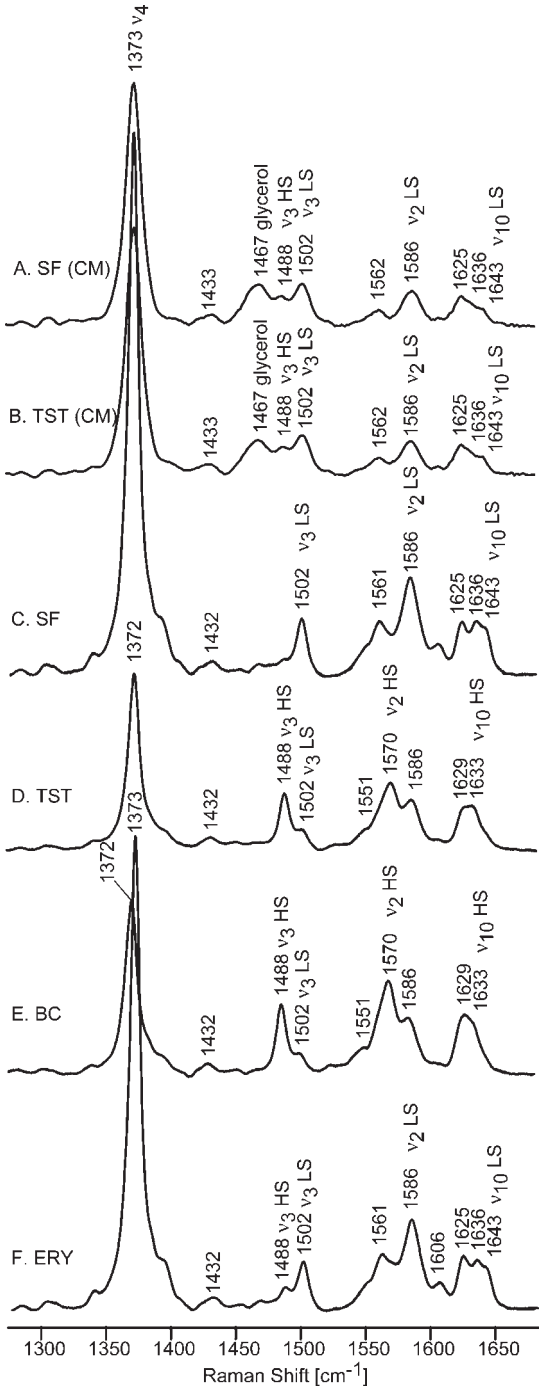

Figure 3. The high frequency RR spectra of 60 μM ferric cytochrome CYP3A4 in detergent without substrate (A), and with 600 μM testosterone (B), as well as RR spectra of ferric cytochrome 3A4 in nanodiscs (100 μM) without substrate (C), with 1200 μM of testosterone (D), bromocriptine (E), and erythromycin (F). The RR spectra were measured at 30 °C; excitation line 406 nm. Spectra were normalized to the ν_3 mode. The "CM" stands for "conventional media" (traces A and B) as opposed to spectra of protein incorporated in nanodiscs (traces C−F).

P450s,[64] but that the added TST substrate is to some extent blocked from entering the active site, as reflected in the total absence of further conversion to the HS state. The point to be made is that the influence of Emulgen 913 and similar types of

dx.doi.org/10.1021/ja105869p |J. Am. Chem. Soc. 2011, 133, 1357–1366

solubilizing agents can introduce complications in studying the structural effects of physiologically relevant substrates. As can be seen by inspection of the data acquired here (e.g., Figure 3, traces C−F), such complications are largely avoided for the nanodisc-incorporated systems.

2. Effect of Substrate Structure on the Nanodisc-Incorporated Ferric Enzyme

a. High Frequency Resonance Raman Spectra. The high frequency RR spectrum of the substrate-free form of nanodisc-incorporated CYP3A4 (ND:CYP3A4) is presented in Figure 3, trace C, exhibiting core size and spin state markers bands at 1502 cm^{-1} (ν_3), 1568 cm^{-1} (ν_2), and 1643 cm^{-1} (ν_{10}), all being characteristic of a low spin 6-coordinated state (LS6c), consistent with a thiolate ligand coordinated on the proximal heme side and a water molecule on the distal side, as is typical for substrate-free P450s.[18,19,23−25,32] It is emphasized here that, contrary to the samples prepared in detergent solution, this sample is largely LS state (~85%; Table S1). The addition of high concentrations of testosterone (trace D), as well as bromocriptine (trace E), causes significant increases in the HS component, as judged by the strong intensities of the ν_3 mode at 1488 cm^{-1} and the ν_2 mode at 1570 cm^{-1}. On the other hand, the addition of ERY to the SF sample causes only slight spin state changes, the spectra of ERY-bound sample (trace F) looking esentially like that of the substrate-free form, except for a very slightly enchanced HS ν_3 mode at 1488 cm^{-1}. These results are consistent with the UV−vis data showing that the ERY-bound ND:CYP3A4 samples are only about 20% high spin state.[51]

Returning attention to the results for the TST and BC-bound forms, as shown in Table S1, the apparent HS population of the TST-bound form is 75%, while that of the BC-bound form is 80%. It is noted that these values are slightly lower than those previously reported for 1 μM ND:CYP3A4 samples containing 1 μM BC and high concentrations of TST. As is explained further in the Supporting Information, these small apparent discrepancies are most reasonably attributed to the large differences in substrate and protein concentrations, as well as small errors introduced by uncertainties in the relative RR cross sections between the HS and LS bands (see the Supporting Information).

b. Low Frequency Resonance Raman Spectra. The low frequency RR spectra of ferric samples of substrate-free, BC- and ERY-bound, as well as that of a sample containing a large amount of TST (1200 μM) are shown in Figure 4. The low frequency spectrum of substrate-free ND:CYP3A4 (Figure 4, trace A) exhibits two modes associated with "propionate bending" at 370 and 378 cm^{-1}, and two modes assigned to "vinyl bending" modes, a lower intensity one at 411 cm^{-1} and higher intensity mode at 423 cm^{-1}; the quotation marks are included in these descriptions in compliance with more recent studies that have documented involvement of other pyrrole substituents, as reflected in the rather substantial isotopic shifts observed upon deuteration of the peripheral methyl groups.[66,67]

The addition of BC or high concentrations of TST, which caused substantial changes in spin-state marker modes, leads to small, but definite, changes in the modes associated with heme peripheral group dispositions or out-of-plane macrocycle distortion. Thus, the traces for TST and BC bound samples exhibit only slight increases in the intensities of the out-of-plane heme modes observed near 315−330 cm^{-1} and at ~500 cm^{-1}. Similarly, binding of substrate seems to induce a rather small decrease of the lower frequency propionate bending mode near 370 cm^{-1} and a corresponding increase in the stronger propionate mode at

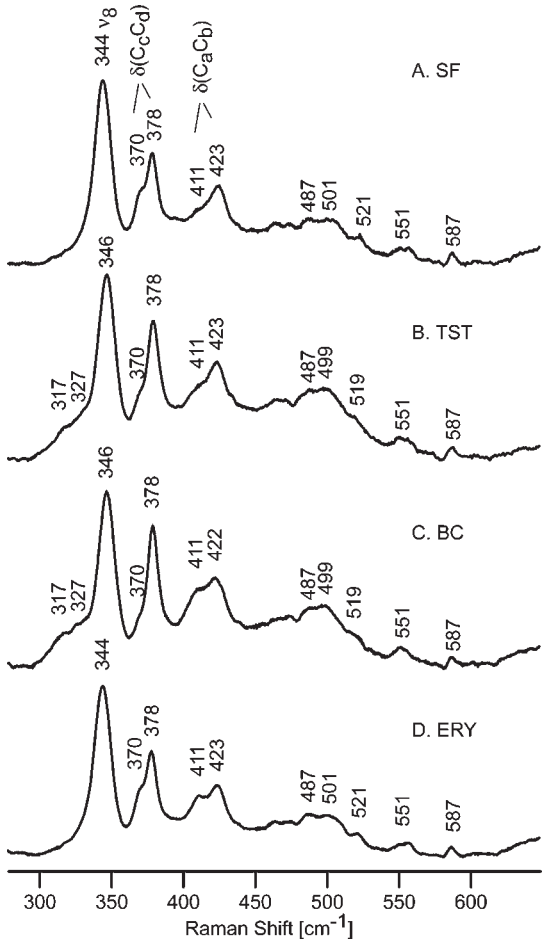

Figure 4. The low frequency RR spectra of ferric cytochrome 3A4 in nanodiscs without substrate (A), with 1200 μM of testosterone (B), bromocriptine (C), and erythromycin (D). The RR spectra were measured at 30 °C; excitation line 406 nm. Spectra were normalized to the ν_8 mode.

378 cm^{-1}; it is interesting to note that this effect on propionate modes is opposite of that observed for bacterial P450s, where binding of substate led to activation of the lower frequency propionate bending mode.[23,25] The only obvious effect on the vinyl modes is that the substrate-bound forms seem to have larger intensities in the lower frequency component (near 410 cm^{-1}) as compared to the feature near 420 cm^{-1}. The binding of ERY does not induce any detectable enhancement of out-of-plane modes, but slightly increases the lower frequency vinyl bending mode intensity, relative to the 423 cm^{-1} feature.

3. Effects of Loading of Smaller Substrates on Ferric CYP3A4.

Inasmuch as it has been shown that up to three testosterone molecules can bind within the large distal pocket of CYP3A4,[46,50] it is of interest to probe this system at different levels of TST loading so as to provide an evaluation of the effect of pocket crowding on heme structure. As is shown in Figures S1 and S2 of the Supporting Information, while addition of increasing concentrations of TST causes HS markers and low frequency oop modes to increase and LS markers to decrease, there is no evidence for more than one type of HS component. Thus, the results obtained argue that one molecule of TST is apparently insufficient to trigger a spin state conversion, two bound TST molecules generate a substantial HS population, which is further populated by the third TST without causing any further distinct heme structural changes.

dx.doi.org/10.1021/ja105869p | J. Am. Chem. Soc. 2011, 133, 1357–1366

B. Ferrous CO P450 3A4 and Its Interaction with Substrates. The RR spectra of relatively stable ferrous CO adducts of cytochrome P450 provide useful information about distal side pocket structure and ligand protein interactions. Moreover, the changes in the modes associated with the Fe−C−O fragment reflect not only strength of the proximal trans ligand, but also the polarity of the distal pocket environment, such as H-bond interaction with the distal amino acids, water molecules, or substrates. It is well-known that back-donation of the Fe(II) d_π electrons to ligands π^* orbitals increases the Fe−C while weakening the C−O bond strengths, resulting in a negative linear correlation between the C−O and Fe−C stretching frequencies.[18,19,29−32,35] The ν(Fe−C) and ν(C−O) stretching modes are usually observed in the regions of 460−490 and 1920−1970 cm^{-1}, respectively, while the δ(Fe−C−O) bending mode is seen at around 560−570 cm^{-1}.[18,19,29−32,35] The spectra of ferrous CO samples were measured with the 442 nm excitation line at 4 °C; in all cases, there were no observed differences in the spectra measured at 4 and 30 °C.

1. Effect of Substrate Structure on the Ferrous CO Adducts. The oxidation and spin-state marker bands of these low spin 6-coordinate CO adducts occur at virtually identical positions, regardless of substrate occupation, as expected (Figure S3, Supporting Information); that is, the ν_4 mode is located at 1371 cm^{-1}, the ν_3 mode at 1496 cm^{-1}, and the ν_2 mode at 1586 cm^{-1}. In accordance with this observation, it is also seen by inspection of Figure 5 that there are no significant effects of substrate binding or substrate structure on the low frequency heme modes that occur between 200 and 850 cm^{-1}. However, substrate binding does have a definite impact on the disposition of the Fe−C−O fragment, as judged by obvious changes in its vibrational parameters; that is, the ν(Fe−C) modes shift between 476 and 491 cm^{-1} and in certain cases appear to be asymmetric, implying the existence of two or more conformers. To evaluate these possibilities, the low frequency spectra were deconvoluted and supplemented by spectra acquired between 1800 and 2100 cm^{-1}, where corresponding ν(C−O) modes are expected to occur, these spectra being displayed in Figure 6.

In the low frequency spectrum of the substrate-free sample, the asymmetric peak at around 476 cm^{-1} is fit best with two peaks of 23 cm^{-1} bandwidth corresponding to two ν(Fe−C) conformers positioned at 476 and 491 cm^{-1} (Figure 6, trace A). This assignment is supported by the observation of two ν(C−O) stretches in the high frequency region, at 1929 and 1953 cm^{-1} (inset of trace A). It is also important to note that the relative intensities of these modes are well correlated; that is, the modes at 476 and 1953 cm^{-1} are more intense and represent one Fe−CO conformer, while the less intense pair of modes at 491 and 1929 cm^{-1} corresponds to the second conformer.

Upon binding the relatively large BC substrate, it appears that only one conformer is generated; that is, the feature observed at 484 cm^{-1} is fitted well with only one peak, whose 23 cm^{-1} bandwidth is consistent with those seen for the two conformers of the substrate-free form. Again, this interpretation is clearly supported by the observation of a single ν(C−O) mode appearing at 1935 cm^{-1}. The presence of only one mode in BC-bound sample implies that this substrate occupies a large portion of heme pocket, permitting only one Fe−C−O conformer. The spectra of ERY-bound sample also show only one ν(Fe−C) stretch occurring at 479 cm^{-1} and its corresponding single ν(C−O) mode at 1948 cm^{-1}. Interesting aspects of this ν(Fe−C) mode of the ERY-bound sample are that it possesses a very narrow bandwidth (14 cm^{-1}) and exhibits a remarkably high intensity, being comparable to the intense ν_7 mode (Figure 5, trace D). The narrowing and high intensity of this mode is possibly associated with a very rigid conformation of the Fe−CO fragment and possible hydrogen bonding to the ERY substrate, a suggestion that is consistent with previously reported X-ray crystallographic data.[68]

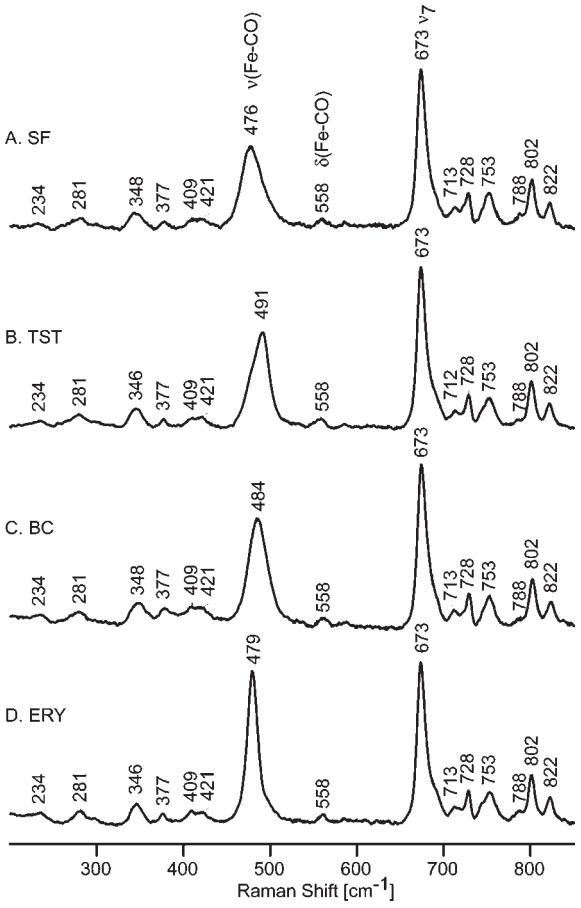

Figure 5. The low frequency RR spectra of ferrous CO adducts of cytochrome 3A4 in nanodiscs without substrate (A), with 1200 μM of testosterone (B), bromocriptine (C), and erythromycin (D). The RR spectra were measured at 4 °C; excitation line 442 nm. Spectra were normalized to the ν_7 mode.

2. Effect of Substrate Loading on Ferrous CO Adducts. Also shown in Figure 6 are the spectra of ND:P4503A4 with different loadings of TST. The ν(Fe−C) envelope observed for the 130 μM TST sample (Figure 6, trace D) is very wide and asymmetric, requiring application of the deconvolution procedures. Inasmuch as the corresponding ν(C−O) modes are seen at the same frequencies observed for the substrate-free form (i.e., at 1929 and 1953 cm^{-1}), it was deemed most appropriate to also use the same initial ν(Fe−C) frequencies observed for the substrate-free form and then attempt different fitting strategies. First, the frequencies and intensities were allowed to vary, while holding the bandwidths constant, the net result being that a satisfactory fit was not attainable. On the other hand, when the frequencies were held constant, allowing the intensities and bandwidths to vary, a satisfactory fit was quickly attained, yielding two ν(Fe−C) modes having bandwidths of 23 and 17 cm^{-1} for the 476 and 491 cm^{-1} features, respectively; that is, a selective narrowing of the high frequency component was observed.

dx.doi.org/10.1021/ja105869p | J. Am. Chem. Soc. 2011, 133, 1357–1366

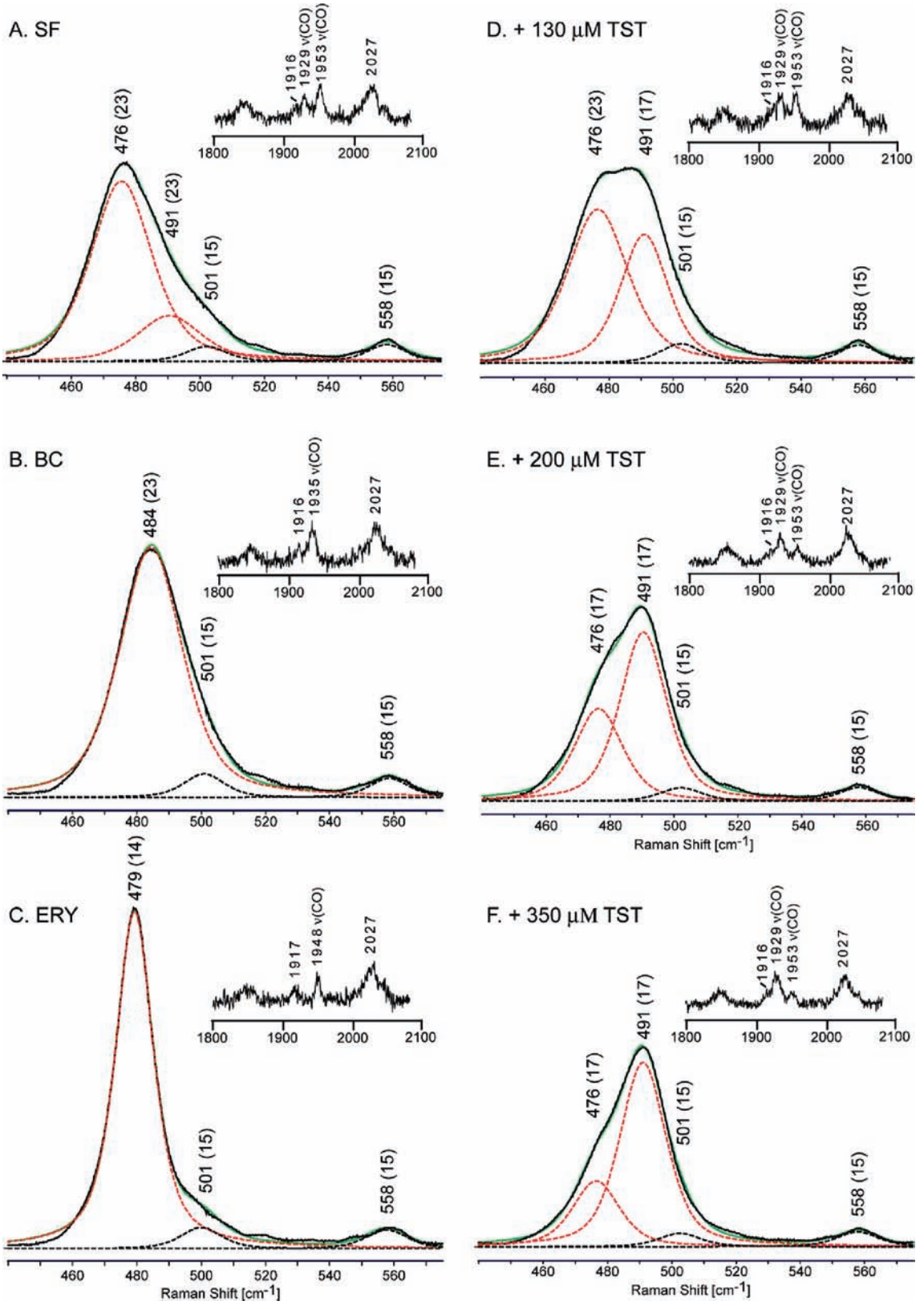

Figure 6. High-resolution low frequency RR spectra of ferrous CO adducts of cytochrome 3A4 in nanodiscs without substrate (A), with 200 μM bromocriptine (B), with 800 μM erythromycin (C), with 130 μM of testosterone (D), with 200 μM of testosterone (D), and with 350 μM of testosterone (E). Note the samples with 350, 600, and 1200 μM of testosterone give the same spectra. The RR spectra were measured at 4 °C; excitation line 442 nm. Spectra were normalized to the ν_7 mode and deconvoluted as described in text. Black solid line, experimental data; green solid line, fitted spectra; red dotted line, modes associated with ν(Fe−CO) modes; black dotted line, other modes in this region. The insets show the high frequency region of corresponding samples.

dx.doi.org/10.1021/ja105869p |*J. Am. Chem. Soc.* 2011, 133, 1357–1366

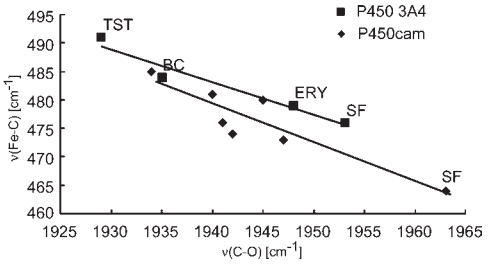

Figure 7. The inverse correlation between the ν(Fe−C) and ν(C−O) frequencies. The "■" represent points for the ND:CYP3A4, and the "◆" are for the CYP101 proteins (from refs 31,32,69−71).

The addition of TS to a total of 200 μM caused further increases in the relative intensity of the higher frequency component, noting the interesting fact that a satisfactory fit could only be obtained by permitting a comparably narrow bandwidth to the lower frequency Fe−C mode. Further additions of TST to 350 μM yielded higher percentages of the 491 cm^{-1} component, but no further narrowing of either feature. Finally, it is emphasized that the observed intensity variations of the corresponding ν(C−O) modes upon loading of TST are entirely consistent with the parameters extracted from the low frequency deconvolution procedure. These observations lead to the conclusion that higher TST loadings reduce, although not completely eliminate, the population of Fe−CO conformer that is dominant in the substrate-free form. Furthermore, the apparently crowded distal pocket leads to more restricted conformations, as reflected in the narrower bandwidths observed at higher loadings of TST.

Plots of the ν(C−O) versus the ν(Fe−C) frequencies represent the FeCO backbonding correlation and provide very useful information, not only about proximal ligand effects, but also the distal heme pocket environment, including steric distortions of the Fe−C−O fragment and polarity of the distal heme pocket. It is generally accepted that a positive polar distal environment, including H-bonding, causes lowering of the ν(CO) and a corresponding increase of the ν(Fe−C) frequency, yielding points to the left side of the correlation. As shown in Figure 7, the ν(C−O)/ν(Fe−C) points observed for the ND:CYP3A4 preparations studied here document increases in positive polarity upon binding of various substrates. Behavior similar to this has been observed for CYP101, as shown in the lower correlation line in Figure 7, and interpreted as being indicative of H-bond formation with distal pocket Thr and Asp residues upon exclusion of the distal pocket water clusters present in the substrate-free form.[31,32,69−72] Addition of BC and TST substrates to the ND:CYP3A4 samples results in more polar environments in the vicinity of the Fe−CO fragment, with the TST having the strongest effect. Binding of the ERY substrate leads to formation of an apparently weaker, but highly directed H-bonding interaction that results in narrow and intense ν(Fe−C) and ν(C−O) features. The observed ability of this protein to accommodate three such structurally different substrates reflects the anticipated flexibility of the large distal pocket. On the other hand, the observed differential effects of these substrates on the vibrational parameters (disposition) of the Fe−CO fragment imply that the structure of substrate can indeed impact the CYP3A4 reactivity and function.

■ CONCLUSIONS

Several important findings have emerged from the present work. First, the use of the nanodisc sampling methodology, which had previously been shown to elicit more well-behaved functional properties, is now shown to lead to a system with well-defined spectral parameters that are indeed responsive to substrate binding in a manner that is consistent with observed functional changes. The binding of TST in high concentrations, as well as binding of BC, result in large spin shifts, while binding of ERY causes only a slight spin shift. In the low frequency region, there are only minor changes in the modes associated with out-of-plane macrocycle distortion or heme peripheral group dispositions, a finding that contrasts with the behavior typically observed for bacterial P450s. Significantly, although several new RR features associated with out-of-plane or peripheral group bending modes appear in the LF spectral region when TST is added, it is noted that there is apparently only one type of high-spin state, whose structure is not sensitive to the number of bound TST molecules.

Although there are no noticeable effects of substrate structure or loading on the heme spectral features, there are definite differences observed for the modes associated with the Fe−CO fragment, with shifts of up to 15 cm^{-1} being seen. This strong effect of some substrates on the vibrational spectra of Fe−CO unit in cytochromes P450 is usually attributed to the steric and/or electronic perturbation caused by interactions with the bound ligand. While comparable shifts upon substrate binding are commonly observed for bacterial P450s,[18,19,25] they are generally not seen for most mammalian cytochromes P450, when studied in conventional media; for example, very small effects on the vibrational modes of the Fe−C−O fragments were observed for CYP2B4 upon binding of substrates.[24] Although it is true that relatively large changes in the Fe−C and C−O stretching modes have been reported for the CO adduct of CYP19 upon binding of its substrate, 19-oxo androstenedione,[73] it is noted that this is a type of steriodogenic cytochrome P450 that typically exhibits high sterospecificity, implying a tightly organized binding site more similar to those of bacterial P450s.

■ ASSOCIATED CONTENT

Supporting Information. Table with summary of calculated spin state distributions for CYP3A4 samples, figures of high and low frequency resonance Raman spectra of ferric ND:CYP3A4 with different concentrations of TST, and high frequency RR spectra of ferrous CO adducts of ND:CYP3A4 with different substrates. This material is available free of charge via the Internet at http://pubs.acs.org.

■ AUTHOR INFORMATION

Corresponding Author

s-sligar@illinois.edu; james.kincaid@marquette.edu

■ ACKNOWLEDGMENT

This work was supported by National Institutes of Health grants GM31756 and GM33775 to S.G.S. and DK 35153 to J.R.K.

■ REFERENCES

(1) Guengerich, F. P. In *Cytochrome P450: Structure, Mechanism, and Biochemistry*; Ortiz de Montellano, P. R., Ed.; Kluwer Academics/Plenum Publisher: New York, 2005; pp 377−530.

(2) Sigel, A., Sigel, H., Sigel, R. K. O., Eds. *Metal Ions in Life Sciences*; John Wiley & Sons, Ltd.: New York, 2007; Vol. 3.

(3) Guengerich, F. P. *Annu. Rev. Pharmacol. Toxicol.* **1999,** *39*, 1–17.
(4) Davydov, D. R.; Halpert, J. R. *Expert Opin. Drug Metab. Toxicol.* **2008,** *4*, 1523–1535.
(5) Denisov, I. G.; Frank, D. J.; Sligar, S. G. *Pharmacol. Ther.* **2009,** *124*, 151–167.
(6) Frank, D. J.; Denisov, I. G.; Sligar, S. G. *Arch. Biochem. Biophys.* **2009,** *488*, 146–152.
(7) Atkins, W. M. *Expert Opin. Drug Metab. Toxicol.* **2006,** *2*, 573–579.
(8) Scott, E. E.; Halpert, J. R. *Trends Biochem. Sci.* **2005,** *30*, 5–7.
(9) Zhou, S.-F. *Curr. Drug Metab.* **2008,** *9*, 310–322.
(10) Williams, P. A.; Cosme, J.; Vinkovic, D. M.; Ward, A.; Angove, H. C.; Day, P. J.; Vonrhein, C.; Tickle, I. J.; Jhoti, H. *Science* **2004,** *305*, 683–686.
(11) Yano, J. K.; Wester, M. R.; Schoch, G. A.; Griffin, K. J.; Stout, C. D.; Johnson, E. F. *J. Biol. Chem.* **2004,** *279*, 38091–38094.
(12) Ekroos, M.; Sjoegren, T. *Proc. Natl. Acad. Sci. U.S.A.* **2006,** *103*, 13682–13687.
(13) Guengerich, F. P. *Proc. Natl. Acad. Sci. U.S.A.* **2006,** *103*, 13565–13566.
(14) Kijac, A. Z.; Li, Y.; Sligar, S. G.; Rienstra, C. M. *Biochemistry* **2007,** *46*, 13696–13703.
(15) Fishelovitch, D.; Hazan, C.; Shaik, S.; Wolfson, H. J.; Nussinov, R. *J. Am. Chem. Soc.* **2007,** *129*, 1602–1611.
(16) Fishelovitch, D.; Hazan, C.; Hirao, H.; Wolfson, H. J.; Nussinov, R.; Shaik, S. *J. Phys. Chem.* **2007,** *111*, 13822–13832.
(17) Shaik, S.; Cohen, S.; Wang, Y.; Chen, H.; Kumar, D.; Thiel, W. *Chem. Rev.* **2010,** *110*, 949–1017.
(18) Spiro, T. G. In *Biological Applications of Raman Spectroscopy*; Spiro, T. G., Ed.; John Wiley and Sons: New York, 1988; Vol. III.
(19) Kincaid, J. R. In *The Porphyrin Handbook*; Kadish, K. M., Smith, K. M., Guilard, R., Eds.; Academic Press: New York, 2000; Vol. 7, pp 225−291.
(20) Cerda-Colon, J. F.; Silfa, E.; Lopez-Garriga, J. *J. Am. Chem. Soc.* **1998,** *120*, 9312–9317.
(21) Marzocchi, M. P.; Smulevich, G. *J. Raman Spectrosc.* **2003,** *34*, 725–736.
(22) Peterson, E. S.; Friedman, J. M.; Chien, E. Y. T.; Sligar, S. G. *Biochemistry* **1998,** *37*, 12301–12319.
(23) Chen, Z.; Ost, T. W. B.; Schelvis, J. P. M. *Biochemistry* **2004,** *43*, 1798–1808.
(24) Mak, P. J.; Im, S.-C.; Zhang, H.; Waskell, L. A.; Kincaid, J. R. *Biochemistry* **2008,** *47*, 3950–3963.
(25) Mak, P. J.; Kaluka, D.; Manyumwa, E. M.; Zhang, H.; Deng, T.; Kincaid, J. R. *Biopolymers* **2008,** *89*, 1045–1053.
(26) Lee, K. B.; Jun, E.; La Mar, G. N.; Rezzano, I. N.; Pandey, R. K.; Smith, K. M.; Walker, F. A.; Buttlaire, D. H. *J. Am. Chem. Soc.* **1991,** *113*, 3576–3583.
(27) Reid, L. S.; Lim, A. R.; Mauk, A. G. *J. Am. Chem. Soc.* **1986,** *108*, 8197–8201.
(28) Funk, W. D.; Lo, T. P.; Mauk, M. R.; Brayer, G. D.; MacGillivray, R. T. A.; Mauk, A. G. *Biochemistry* **1990,** *29*, 5500–5508.
(29) Yu, N.-T.; Kerr, E. A. In *Biological Applications of Raman Spectroscopy*; Spiro, T. G., Ed.; Wiley & Sons: New York, 1988; Vol. III, pp 39−95.
(30) Ibrahim, M.; Xu, C.; Spiro, T. G. *J. Am. Chem. Soc.* **2006,** *128*, 16834–16845.
(31) Uno, T.; Nishimura, Y.; Makino, R.; Iizuka, T.; Ishimura, Y.; Tsuboi, M. *J. Biol. Chem.* **1985,** *260*, 2023–2026.
(32) Wells, A. V.; Li, P.; Champion, P. M.; Martinis, S. A.; Sligar, S. G. *Biochemistry* **1992,** *31*, 4384–4393.
(33) Deng, T.-J.; Macdonald, I. D. G.; Simianu, M. C.; Sykora, M.; Kincaid, J. R.; Sligar, S. G. *J. Am. Chem. Soc.* **2001,** *123*, 269–278.
(34) Deng, T.-J.; Proniewicz, L. M.; Kincaid, J. R.; Yeom, H.; Macdonald, I. D. G.; Sligar, S. G. *Biochemistry* **1999,** *38*, 13699–13706.
(35) Mak, P. J.; Zhang, H.; Hollenberg, P. F.; Kincaid, J. R. *J. Am. Chem. Soc.* **2009,** *132*, 1494–1495.
(36) Macdonald, I. D. G.; Sligar, S. G.; Christian, J. F.; Unno, M.; Champion, P. M. *J. Am. Chem. Soc.* **1999,** *121*, 376–380.
(37) Hu, S.; Schneider, A.; Kincaid, J. R. *J. Am. Chem. Soc.* **1991,** *113*, 4815–4822.
(38) Ibrahim, M.; Denisov, I. G.; Makris, T. M.; Kincaid, J. R.; Sligar, S. G. *J. Am. Chem. Soc.* **2003,** *125*, 13714–13718.
(39) Ibrahim, M.; Kincaid, J. R. *J. Porphyrins Phthalocyanines* **2004,** *8*, 215–225.
(40) Mak, P. J.; Denisov, I. G.; Victoria, D.; Makris, T. M.; Deng, T.-J.; Sligar, S. G.; Kincaid, J. R. *J. Am. Chem. Soc.* **2007,** *129*, 6382–6383.
(41) Denisov, I. G.; Mak, P. J.; Makris, T. M.; Sligar, S. G.; Kincaid, J. R. *J. Phys. Chem. A* **2008,** *112*, 13172–13179.
(42) Mak, P. J.; Kincaid, J. R. *J. Inorg. Biochem.* **2008,** *102*, 1952–1957.
(43) Davydov, D. R.; Fernando, H.; Baas, B. J.; Sligar, S. G.; Halpert, J. R. *Biochemistry* **2005,** *44*, 13902–13913.
(44) Nath, A.; Atkins, W. M.; Sligar, S. G. *Biochemistry* **2007,** *46*, 2059–2069.
(45) Sligar, S. G. *Biochem. Biophys. Res. Commun.* **2003,** *312*, 115–119.
(46) Baas, B. J.; Denisov, I. G.; Sligar, S. G. *Arch. Biochem. Biophys.* **2004,** *430*, 218–228.
(47) Grinkova, Y. V.; Denisov, I. G.; Waterman, M. R.; Arase, M.; Kagawa, N.; Sligar, S. G. *Biochem. Biophys. Res. Commun.* **2008,** *372*, 379–382.
(48) Denisov, I. G.; Grinkova, Y. V.; McLean, M. A.; Baas, B. J.; Sligar, S. G. *J. Biol. Chem.* **2007,** *282*, 26865–26873.
(49) Denisov, I. G.; Baas, B. J.; Grinkova, Y. V.; Sligar, S. G. *J. Biol. Chem.* **2007,** *282*, 7066–7076.
(50) Nath, A.; Grinkova, Y. V.; Sligar, S. G.; Atkins, W. M. *J. Biol. Chem.* **2007,** *282*, 28309–28320.
(51) Das, A.; Grinkova, Y. V.; Sligar, S. G. *J. Am. Chem. Soc.* **2007,** *129*, 13778–13779.
(52) Rivory, L. P.; Slaviero, K. A.; Hoskins, J. M.; Clarke, S. J. *Clin. Pharmacokinet.* **2001,** *40*, 151–158.
(53) Gillam, E. M. J.; Baba, T.; Kim, B. R.; Ohmori, S.; Guengerich, F. P. *Arch. Biochem. Biophys.* **1993,** *305*, 123–131.
(54) Domanski, T. L.; Liu, J.; Harlow, G. R.; Halpert, J. R. *Arch. Biochem. Biophys.* **1998,** *350*, 223–232.
(55) Denisov, I. G.; Grinkova, Y. V.; Baas, B. J.; Sligar, S. G. *J. Biol. Chem.* **2006,** *281*, 23313–23318.
(56) Bayburt, T. H.; Grinkova, Y. V.; Sligar, S. G. *Nano Lett.* **2002,** *2*, 853–856.
(57) Bayburt, T. H.; Sligar, S. G. *Proc. Natl. Acad. Sci. U.S.A.* **2002,** *99*, 6725–6730.
(58) Bayburt, T. H.; Sligar, S. G. *Protein Sci.* **2003,** *12*, 2476–2481.
(59) Duan, H.; Civjan, N. R.; Sligar, S. G.; Schuler, M. A. *Arch. Biochem. Biophys.* **2004,** *424*, 141–153.
(60) Bayburt, T. H.; Leitz, A. J.; Xie, G.; Oprian, D. D.; Sligar, S. G. *J. Biol. Chem.* **2007,** *282*, 14875–14881.
(61) Denisov, I. G.; Grinkova, Y. V.; Lazarides, A. A.; Sligar, S. G. *J. Am. Chem. Soc.* **2004,** *126*, 3477–3487.
(62) McKenna, C. E.; Gutheil, W. G.; Song, W. *Biochim. Biophys. Acta* **1991,** *1075*, 109–117.
(63) Shriver, D. F.; Dunn, J. B. R. *Appl. Spectrosc.* **1974,** *28*, 319–323.
(64) Hosea, N. A.; Guengerich, F. P. *Arch. Biochem. Biophys.* **1998,** *353*, 365–373.
(65) Davydov, D. R.; Baas, B. J.; Sligar, S. G.; Halpert, J. R. *Biochemistry* **2007,** *46*, 7852–7864.
(66) Mak, P. J.; Podstawka, E.; Kincaid, J. R.; Proniewicz, L. M. *Biopolymers* **2004,** *75*, 217–228.
(67) Podstawka, E.; Mak, P. J.; Kincaid, J. R.; Proniewicz, L. M. *Biopolymers* **2006,** *83*, 455–466.
(68) Nagano, S.; Cupp-Vickery, J. R.; Poulos, T. L. *J. Biol. Chem.* **2005,** *280*, 22102–22107.
(69) Jung, C.; Hui Bon Hoa, G.; Schroeder, K. L.; Simon, M.; Doucet, J. P. *Biochemistry* **1992,** *31*, 12855–12862.

(70) Hu, S.; Kincaid, J. R. *J. Am. Chem. Soc.* **1991,** *113*, 2843–2850.
(71) Bangcharoenpaurpong, O. Ph.D. Dissertation, Northeastern University, Boston, MA, 1987.
(72) Spiro, T. G.; Wasbotten, I. H. *J. Inorg. Biochem.* **2005,** *99*, 34–44.
(73) Tosha, T.; Kagawa, N.; Ohta, T.; Yoshioka, S.; Waterman, M. R.; Kitagawa, T. *Biochemistry* **2006,** *45*, 5631–5640.